THE ASTROPHYSICAL JOURNAL, 595:L29–L32, 2003 September 20
© 2003. The American Astronomical Society. All rights reserved. Printed in U.S.A.

DELAYED SOFT X-RAY EMISSION LINES IN THE AFTERGLOW OF GRB 030227

D. WATSON,[1] J. N. REEVES,[2,3] J. HJORTH,[1] P. JAKOBSSON,[1] AND K. PEDERSEN[1]

Received 2003 June 13; accepted 2003 August 4; published 2003 August 21

ABSTRACT

Strong delayed X-ray line emission is detected in the afterglow of gamma-ray burst GRB 030227, appearing near the end of the *XMM-Newton* observation, nearly 20 hr after the burst. The observed flux in the lines, not simply the equivalent width, sharply increases from an undetectable level ($<1.7 \times 10^{-14}$ ergs cm^{-2} s^{-1}, 3 σ) to $4.1^{+0.9}_{-1.0} \times 10^{-14}$ ergs cm^{-2} s^{-1} in the final 9.7 ks. The line emission alone has nearly twice as many detected photons as any previous detection of X-ray lines. The lines correspond well to hydrogen- and/or helium-like emission from Mg, Si, S, Ar, and Ca at a redshift $z = 1.39^{+0.03}_{-0.06}$. There is no evidence for Fe, Co, or Ni—the ultimate iron abundance must be less than a tenth that of the lighter metals. If the supernova and GRB events are nearly simultaneous, there must be continuing sporadic power output after the GRB of a luminosity $\gtrsim 5 \times 10^{46}$ ergs s^{-1}, exceeding all but the most powerful quasars.

Subject headings: gamma rays: bursts — supernovae: general — X-rays: general

1. INTRODUCTION

Analysis of the afterglows of long-duration gamma-ray bursts (GRBs) has finally shown their progenitors to be massive stars (Reeves et al. 2002; Paczyński 1998; Galama et al. 1998), with a catastrophic endpoint that seems to produce both a GRB and a supernova (SN; Bloom et al. 1999; Hjorth et al. 2003; Price et al. 2003). Rapid follow-up observations of GRBs at X-ray energies have provided spectra of the afterglows showing very high luminosity line emission. Initially, single emission lines believed to be Fe (Antonelli et al. 2000; Piro et al. 1998, 2000; Yoshida et al. 2001) or Ni (Watson et al. 2002a) were reported and more recently, transient multiple emission lines from highly ionized Si, S, Ar, Ca, and possibly Mg and Ni (Reeves et al. 2002). Analysis of the *Chandra* grating spectra of the afterglow of GRB 020813 has indicated the presence of highly ionized states of similar low-Z metals, in particular S and Si at much lower equivalent widths than observed in GRB 011211 (Butler et al. 2003).

2. OBSERVATIONS AND DATA REDUCTION

XMM-Newton (Jansen et al. 2001) began observing the error-box of GRB 030227 8 hr after the burst (for 13 hr), and for the first time a GRB detected by the *International Gamma-Ray Astrophysical Laboratory* (*INTEGRAL*; Parmar et al. 2003) was localized to within a few arcseconds (Loiseau et al. 2003). Three exposures were made with the European Photon Imaging Camera (EPIC), the first two interrupted by high background events. The effective time of the first exposure was less than 1 ks and is contaminated by high particle background; it was therefore not considered for spectral analysis. Data from the MOS and pn cameras are consistent, allowing for cross-calibration uncertainties of $\lesssim$15% between the instruments. Because of the extra free parameters introduced by allowing for systematic differences between instruments and the much greater sensitivity of the EPIC-pn detector, the pn data were used for spectral fitting. The final fit results were then checked against the MOS data and found to be consistent.

The data reduction followed a standard procedure similar to that outlined in Watson et al. (2002b), except that the data were processed and reduced with the *XMM-Newton* SAS version 5.4.1. A spectral binning using a minimum of 20 counts per bin was used. Consistent results were obtained using minima of 10, 12, 20, and 25 counts per bin, as expected (Yaqoob 1998), and using background spectra from different regions on the detector.

The data were divided into four time segments to examine spectral evolution. The first segment corresponded to the second exposure, the remaining three comprising consecutive 10, 10, and 11 ks parts of the third exposure, giving respective exposure times of 5.7, 8.7, 9.0, and 9.7 ks. In this Letter, quoted errors are 90% confidence intervals, unless stated otherwise.

3. RESULTS: SPECTRAL EMISSION FEATURES

This is the first afterglow discovered for an *INTEGRAL* GRB and had an average 0.2–10.0 keV flux of $8.7^{+0.7}_{-1.3} \times 10^{-13}$ ergs cm^{-2} s^{-1}, decaying with a power-law slope of -1.0 ± 0.1 with no strong evidence for deviations from this decay rate (see Mereghetti et al. 2003).

The complete spectrum of the afterglow and each time segment individually can be fitted with a power law and require absorption well in excess of the Galactic value, with absorption consistently around twice the Galactic foreground column density (the Galactic hydrogen absorbing column in this direction is 22×10^{20} cm^{-2}, although the uncertainty on this value may be as large as 50%; Dickey & Lockman 1990).

However, the spectrum evolves during the observation, showing emission lines (see Fig. 1) at observed energies of $0.62^{+0.03}_{-0.02}$, $0.86^{+0.02}_{-0.03}$, 1.11 ± 0.02, $1.35^{+0.04}_{-0.03}$, and 1.67 ± 0.04 keV only in the final ~10 ks, approximately 70 ks after the GRB.

The absorbed power-law fit (χ^2/degrees of freedom [dof] = 85.2/71) is clearly improved in the last segment by the addition of the line emission (Fig. 2): adding five narrow Gaussian emission lines (with energy and flux as free parameters) to a power law with variable slope, normalization, and absorption gave an improvement in the fit of $\Delta\chi^2 = 33.3$, corresponding to a null hypothesis probability of 0.04%. Table 1 contains the individual best-fit line parameters and significances.

Since four spectra were examined, a conservative estimate of the significance of these line features is given by the F-test

[1] Astronomical Observatory, Niels Bohr Institute for Astronomy, Physics, and Geophysics, University of Copenhagen, Juliane-Maries Vej 30, DK-2100 Copenhagen Ø, Denmark; kp@astro.ku.dk, darach@astro.ku.dk, jens@astro.ku.dk, pallja@astro.ku.dk.

[2] Laboratory for High Energy Astrophysics, NASA Goddard Space Flight Center, Code 662, Greenbelt, MD 20771; jnr@milkyway.gsfc.nasa.gov.

[3] Universities Space Research Association.

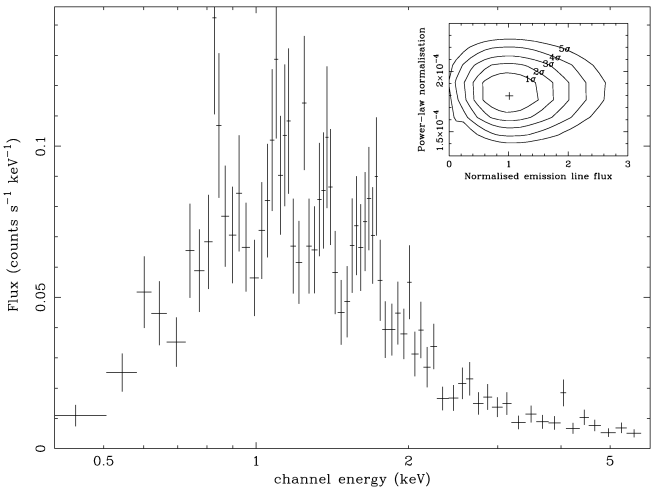

FIG. 1.—EPIC-pn spectrum of the final 9.7 ks exposure of the afterglow of GRB 030227. The effects of the detector response have not been unfolded out of the data; however, the emission lines are still clearly visible between 0.6 and 2 keV. The data are also not fitted in this figure in order not to lead the eye. *Inset*: Statistical confidence contours for the normalized emission-line flux against power-law normalization for five parameters of interest.

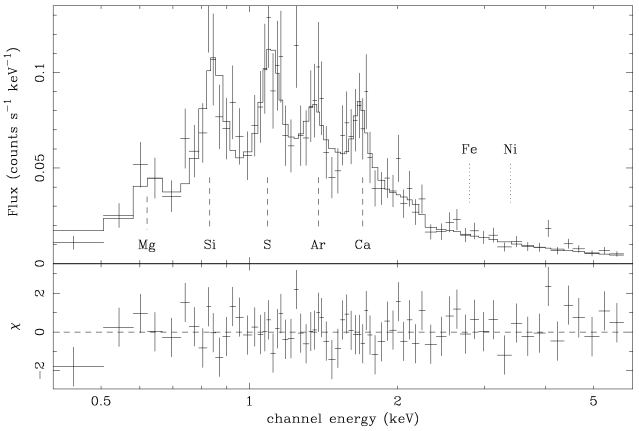

FIG. 2.—EPIC-pn spectrum of the last 11 ks of the afterglow observation. The data are fitted with an absorbed power law and five Gaussian emission lines. The Kα lines of hydrogenic Mg, Si, S, Ar, and Ca, redshifted by $z = 1.39$, are marked with dashed lines. The nominal energies where the Kα lines of hydrogenic Fe and Ni would be expected (also redshifted by $z = 1.39$) are marked with dotted lines. The continuum is smooth at these energies; no Fe, Co, or Ni emission is detected.

probability for the addition of five Gaussian lines to an absorbed power law over four independent trials, which is 0.15% (3.1 σ). A more realistic estimate of the significance is given by a fit to an a priori expected model, i.e., that used by Reeves et al. (2002) to characterize the line emission in GRB 011211. In this model one expects to observe the H-like emission lines of Mg, Si, and S and the He-like lines of Ar and Ca at an arbitrary redshift. The trial-corrected *F*-test null hypothesis probability from this model is 6×10^{-5} (4.0 σ). Finally, one can search the parameter space directly for the error on the total line flux, for the relevant parameters of interest (power-law normalization and slope, absorption, redshift, and total emission-line flux), yielding a probability of 3×10^{-7} or 4.7 σ (4.4 σ for four trials) for zero emission-line flux (see inset in Fig. 1).

3.1. *Comparison with Previous X-Ray Emission Lines*

The detection of soft X-ray line emission in GRB 011211 has been criticized on the basis of possible systematic errors (Borozdin & Trudolyubov 2003) and the level of statistical significance (Rutledge & Sako 2003). Two later reanalyses of the data have been unable to reproduce the systematic problem (Reeves et al. 2003; Rutledge & Sako 2003), and it appears to be due to nonstandard event selection by Borozdin & Trudolyubov (2003).[4] Concerns regarding the statistical significance have been addressed by Reeves et al. (2003).

Similar critical analysis has yet to be addressed to other X-ray line detections. An interesting comparison of the line detections made to date is the number of photons detected only in the line emission. For instance, in GRB 991216, ~25 photons (Piro et al. 2000); GRB 000214, ~35 photons (Antonelli et al. 2000); GRB 020813, ~60 photons (Butler et al. 2003); and GRB 011211, ~115 photons (Reeves et al. 2003). In all of these bursts, the number of counts detected per emission line has been ~25–40. In these observations, we detect ~210 line photons, nearly twice as many as in GRB 011211 and nearly an order of magnitude more than GRB 991216; the number of counts for the brighter emission lines here is ~60 each.

[4] We have been able to reproduce the spurious background line found by Borozdin & Trudolyubov (2003) by including bad events, excluded in standard processing, lying on a *vertical* chip edge physically unrelated to the location of the GRB afterglow (which lay near the horizontal chip edge) or the background regions chosen by Reeves et al. (2002).

TABLE 1
BEST-FIT QUANTITIES FOR THE LINE EMISSION

LINE ID (1)	ENERGY (keV) (2)	LINE z (3)	UNABSORBED FLUX ($\times 10^{-14}$ ergs cm^{-2} s^{-1}) (4)	EW (eV) (5)	SIGNIFICANCE % (6)	SIGNIFICANCE σ (7)
Mg XII	$0.62^{+0.03}_{-0.02}$	1.35	$9.1^{+7.9}_{-6.3}$	211^{+182}_{-146}	97	2.2
Si XIV	$0.86^{+0.02}_{-0.03}$	1.32	$4.1^{+2.7}_{-1.8}$	128^{+83}_{-57}	99.98	3.8
S XVI	$1.11^{+0.02}_{-0.02}$	1.34	$2.4^{+0.8}_{-1.0}$	93^{+33}_{-39}	99.96	3.5
Ar XVIII	$1.35^{+0.04}_{-0.03}$	1.44	$0.9^{+0.9}_{-0.6}$	43^{+42}_{-27}	92	1.7
(Ar XVIII)		(1.31)				
Ca XX	$1.66^{+0.04}_{-0.04}$	1.45	$1.3^{+0.6}_{-0.8}$	76^{+36}_{-44}	99	2.5
(Ca XIX)		(1.34)				

NOTE.—Col. (1) lists the probable line identifications. For Ar and Ca, a helium-like ionization state seems more probable, giving a better match to the inferred redshifts (col. [3]) for the lighter elements. Cols. (2), (4), and (5) are the observed line energies, unabsorbed fluxes, and observed equivalent widths, respectively, while cols. (6) and (7) give the statistical significance (percentage probability and equivalent Gaussian standard deviations) of each line detection (based on the *F*-test comparison between the best-fit model with and without the line).

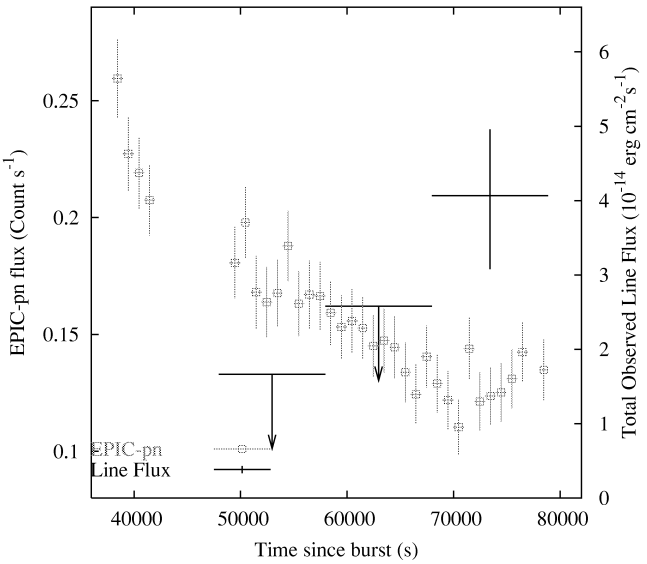

FIG. 3.—EPIC-pn 0.2–10.0 keV light curve for the afterglow of GRB 030227 (*gray, left axis*) and the variation of the total line flux (with 3 σ upper limits) for the longest EPIC-pn exposure (*black, right axis*). The intrinsic flux in the lines increases from an undetectable level and becomes noticeable about 70 ks after the GRB, corresponding to ~27 ks in the progenitor rest frame.

4. PROPERTIES OF THE LINE EMISSION

The lines are remarkably similar to those observed in GRB 011211 (Reeves et al. 2002)—they correspond well to the hydrogen- and helium-like lines of Mg, Si, S, Ar, and Ca. The median redshift of these lines is 1.35, where the ions are assumed to be H-like; however, the ionization states in the heavier elements, Ar and Ca, may be dominated by the He-like ions (see Table 1), resulting in a slightly lower median redshift of 1.34. The redshift determination is robust; the relative line-spacing is correct only for lines due to Mg, Si, S, Ar, and Ca and excludes the possibility of degeneracy in the redshift solution. Previous detections of soft X-ray line emission suggest that the X-ray plasma may flow out at a velocity $\sim 0.1c$ (Reeves et al. 2002; Butler et al. 2003), which is close to that observed in optical GRB outflows (Hjorth et al. 2003). The progenitor redshift is therefore anticipated to be $z \simeq 1.6$.

Line emission alone accounts for about 6% of the total flux in the final 10 ks, which is an unabsorbed flux of 1.8×10^{-13} ergs cm^{-2} s^{-1}. Assuming a redshift of $z = 1.6$ and a flat cosmology where $H_0 = 75$ km s^{-1} Mpc^{-1} and $\Omega_\Lambda = 0.7$, this translates to an isotropic line luminosity of 2.6×10^{45} ergs s^{-1} or a total energy of at least 1×10^{49} ergs, implying that the lower limit to the energy required to produce the lines is $\sim 2 \times 10^{50}$ ergs (Ghisellini et al. 2002), within a factor of 2 of the total gamma-ray energy in the burst (Frail et al. 2001).

4.1. *Iron, Cobalt, and Nickel*

As with GRB 011211, there is no evidence for emission from iron; the 3 σ upper limit to the observed equivalent width for hydrogenic Fe is 175 eV. However, in this afterglow there is no evidence for Ni or Co emission either (equivalent width <140 eV). In order to characterize the relative abundances, a pure (absorbed) collisionally ionized plasma model was fitted (without a power-law component).[5] The best-fit redshift for this model was $z = 1.39^{+0.03}_{-0.06}$. The minimum (3 σ) light metal abundance was 24 times the solar abundance, compared to upper limits of only 1.6 and 18 for Fe and Ni, respectively. The implication of these upper limits is that there is only enough Fe, ^{56}Ni, and ^{56}Co to produce an order of magnitude lower abundance of iron than that found for the lighter metals. This is important, since ^{56}Ni is produced in large quantities in SNe and decays to ^{56}Co and then ^{56}Fe and none of these products is observed. A low abundance of Fe, Co, or Ni is not anticipated in the standard models of GRB progenitors (Pruet, Woosley, & Hoffman 2003; Vietri & Stella 1998), suggesting either (1) a different progenitor, intrinsically poor in iron-group elements, or (2) a bias toward observing emission from the outer layers of the progenitor star and that very little Ni has been dredged up to these layers by turbulent mixing by the time the line emission is excited.

Lazzati, Ramirez-Ruiz, & Rees (2002) suggested that a high Fe abundance may still be present while the Fe Kα emission is suppressed by Auger autoionization. A model based on reflection from an optically thick medium was examined. Available models (e.g., Ballantyne & Ramirez-Ruiz 2001) are dominated by Fe emission, do not include some abundant metals (S, Ar, and Ca), and cannot give a reasonable fit to the data at low energies; however, the model and data were compared at high energies. One can indeed strongly depress the Fe Kα lines; however, the model cannot fit the continuum at energies above 7 keV (in the rest frame) because of large Fe absorption. It is unlikely that this mechanism can both suppress the Fe or Ni emission and produce a smooth continuum at high energies. We conclude that Si and other α-burning products but not Fe, Co, or Ni must be highly abundant in the line-emitting plasma.

4.2. *Photoionization*

The line emission may result from photo-, rather than collisional, ionization. In this case, the plasma may have quite different properties. A model for a photoionized plasma was developed with XSTAR,[6] allowing variable abundances of the most abundant elements, and was added to the absorbed power-law model and fitted to the data from the final segment of the observation. The data were as well-fitted by this model (χ^2/dof = 59.3/62) as by the collisionally ionized model (χ^2/dof = 61.3/67), although requiring more free parameters. The fit requires a moderately high ionization parameter, $\log \Xi \sim 3$. The best-fit redshift ($1.38^{+0.05}_{-0.03}$) and elemental abundance ratios (high light metal abundances, low Fe) are similar to those derived from the collisionally ionized model above, confirming that these results are independent of the assumed emission model.

5. IMPLICATIONS OF THE DELAY

Line emission is detected only in the final segment of this observation (Fig. 3), implying that the lines fade, as observed in GRB 011211, but also appear some time after the GRB, in this case 6 or 7 hr in the rest frame. There are two explanations for delayed line emission and each specifies both the geometry and the delay in the central power output.

The first involves direct excitation of the lines by the GRB

[5] Adding a power law to the thermal fit does not change the plasma temperature significantly but makes the absolute abundances harder to constrain by adding two extra free parameters; however, the 2 σ Fe abundance upper limit is still an order of magnitude less than the light metal abundance, even after adding an underlying power law to the collisionally ionized plasma model.

[6] See http://heasarc.gsfc.nasa.gov/docs/software/xstar/xstar.html.

event; they must be delayed by taking a much longer path to the observer than the gamma rays (reverberation). In the second case, there must be continuing sporadic injection of energy after the GRB has finished.

In a reverberation-dominated scenario, the minimum distance from the GRB to the line-emitting plasma can be estimated. It is 9×10^{14} cm (where the off-axis angle is 90°). If the plasma is flowing out from the stellar remnant at $\sim 0.1c$ (e.g., Reeves et al. 2002), it implies a delay of at least 3.5 days between the event causing the matter outflow (presumably an SN) and the GRB. If the line emission is produced by the GRB jet itself, the line-emitting plasma must be very near or in the edge of the jet. The off-axis angle must then be much less than 90°, implying a longer time delay between the matter outflow and the GRB. The jet opening angle (and hence the off-axis angle for the material) can be constrained. Using the method of Bloom, Frail, & Sari (2001), the equivalent isotropic energy was derived for this burst (extrapolating the *INTEGRAL*/SPI spectrum) and the actual gamma-ray energy release was assumed to be 5×10^{50} ergs (Frail et al. 2001). The ratio of these numbers implies a half-opening angle of ~15° for the jet. At this angle, the inferred distance is 2×10^{16} cm, implying a delay between the matter expulsion and the GRB of about 80 days. An SN considerably prior to the GRB (e.g., a "supranova") would be a natural interpretation in this scenario (Lazzati 2003). It should be noted that for delay due to reverberation as outlined above, the line-emitting material would have to be enriched in light elements, poor in iron, nickel, and cobalt, and concentrated in dense clumps slightly off-axis from the GRB jet but generally located around this axis, otherwise the total ejected mass is prohibitively large.

Recent observations of a nearby GRB (030329) show evidence of an SN in the optical spectra, constraining the SN-GRB time delay to be less than 3–5 days (Hjorth et al. 2003; Price et al. 2003). If the result is general and all long-duration GRBs have the same progenitors, as appears likely, then the SN-GRB delay required in the reverberation scenario for this burst (described above) disqualifies straightforward reverberation.

An analysis of a different reverberation scenario has been made by Kumar & Narayan (2003), where gamma- and hard X-radiation from the GRB and the early afterglow is reflected back onto the outer layers of the expanding SN. This concept has the advantage that it does not require a delayed two-stage explosion sequence (SN, GRB) to produce the reverberation. Furthermore, it naturally explains the lack of emission from heavier ions (Fe, Co, and Ni) if the outer layers of the SN ejecta are dominated by lighter metals. The principal difficulty, as pointed out by Kumar & Narayan (2003), is that it is hard to produce X-ray line luminosities greater than 10^{48} ergs, as directly observed here.

Finally, we turn to continuing energy injection to explain the delayed X-ray lines. In the collapsar model (MacFadyen & Woosley1999), where the radius of the dense matter must be $\lesssim 10^{13}$ cm (the size of an exploding Wolf-Rayet star) and a single event (the GRB) must produce all the observed features, the reverberation time is too short to account for the observed delay. In order to produce emission lines, it has been proposed (Rees & Mészáros 2000) that a strong post-GRB source is reflected off the internal edges of a cavity evacuated in the star by the GRB jet (Zhang, Woosley, & MacFadyen 2003). The enormous power in the X-ray lines implies that the continuum luminosity onto the cavity edge must, at the very least, be 5×10^{46} ergs s^{-1} for a duration of a few thousand seconds. A source with this luminosity would equal the X-ray afterglow continuum observed here and be clearly detected; the continuum source must therefore be either obscured or intrinsically anisotropic. The more likely proposition is an anisotropic source as expected for a hot accretion disk (Zhang et al. 2003) or a young rapidly accreting pulsar with a strong magnetic field (Rees & Mészáros 2000), both proposed as consequences of a GRB in a massive star. In normal pulsars, the emission axis is offset from the rotation axis, as is required here. A natural corollary of the geometry in the case of the pulsar, if the emission can be restricted to a cone-shaped beam from the poles, is that the inner regions of the cavity wall, where the Fe/Ni abundance can be expected to be highest, may not be illuminated by the pulsar beam, resulting in a light metal-rich but Fe/Ni–deficient X-ray reflection spectrum because of the laminar separation of elements in an aged massive star.

We note that it is also possible to produce the line emission from a (nonequilibrium) collisionally ionized plasma where there is continuous shock-heating of the ejected material. In this case also, continued injection of energy after the GRB seems to be required.

We thank F. Jansen for the allocation of discretionary time, the *XMM-Newton*–SOC team for performing the rapid follow-up observation, and L. Hanlon, D. Lazzati, B. McBreen, and E. Ramirez-Ruiz for discussions. We acknowledge benefits from collaboration within the EU FP5 Research Training Network, "Gamma-Ray Bursts: An Enigma and a Tool." This work was also supported by the Danish Natural Science Research Council (SNF).

REFERENCES

Antonelli, L. A., et al. 2000, ApJ, 545, L39
Ballantyne, D. R., & Ramirez-Ruiz, E. 2001, ApJ, 559, L83
Bloom, J. S., Frail, D. A., & Sari, R. 2001, AJ, 121, 2879
Bloom, J. S., et al. 1999, Nature, 401, 453
Borozdin, K. N., & Trudolyubov, S. P. 2003, ApJ, 583, L57
Butler, N. R., et al. 2003, ApJ, submitted (astro-ph/0303539)
Dickey, J. M., & Lockman, F. J. 1990, ARA&A, 28, 215
Frail, D. A., et al. 2001, ApJ, 562, L55
Galama, T. J., et al. 1998, Nature, 395, 670
Ghisellini, G., Lazzati, D., Rossi, E., & Rees, M. J. 2002, A&A, 389, L33
Hjorth, J., et al. 2003, Nature, 423, 847
Jansen, F., et al. 2001, A&A, 365, L1
Kumar, P., & Narayan, R. 2003, ApJ, 584, 895
Lazzati, D. 2003, A&A, 399, 913
Lazzati, D., Ramirez-Ruiz, E., & Rees, M. J. 2002, ApJ, 572, L57
Loiseau, N., et al. 2003, GCN Circ. 1901 (http://gcn.gsfc.nasa.gov/gcn/gcn3/1901.gcn3)
MacFadyen, A. I., & Woosley, S. E. 1999, ApJ, 524, 262
Mereghetti, S., et al. 2003, ApJ, 590, L73
Paczyński, B. 1998, ApJ, 494, L45
Parmar, A. N., et al. 2003, Proc. SPIE, 4851, 1104
Piro, L., et al. 1998, A&A, 331, L41
———. 2000, Science, 290, 955
Price, P. A., et al. 2003, Nature, 423, 844
Pruet, J., Woosley, S. E., & Hoffman, R. D. 2003, ApJ, 586, 1254
Rees, M. J., & Mészáros, P. 2000, ApJ, 545, L73
Reeves, J. N., Watson, D., Osborne, J. P., Pounds, K. A., & O'Brien, P. T. 2003, A&A, 403, 463
Reeves, J. N., et al. 2002, Nature, 416, 512
Rutledge, R. E., & Sako, M. 2003, MNRAS, 339, 600
Vietri, M., & Stella, L. 1998, ApJ, 507, L45
Watson, D., et al. 2002a, A&A, 393, L1
———. 2002b, A&A, 395, L41
Yaqoob, T. 1998, ApJ, 500, 893
Yoshida, A., et al. 2001, ApJ, 557, L27
Zhang, W., Woosley, S. E., & MacFadyen, A. I. 2003, ApJ, 586, 356